Three-Dimensional Computations of Equivalent Potential Vorticity

DONALD W. MCCANN

Experimental Forecast Facility, National Severe Storms Forecast Center, Kansas City, Missouri

15 August 1994 and 7 June 1995

ABSTRACT

Moore and Lambert showed how a quantity called equivalent potential vorticity (EPV) can provide quantitative values to assess conditional symmetric instability (CSI), also known as slantwise instability. Expanding the EPV equation into three dimensions, the equation becomes a function of the geostrophic wind shear, the horizontal equivalent potential temperature gradient, the absolute geostrophic vorticity, and the vertical equivalent potential temperature gradient, all of which are easily computed from gridded data. The equation reduces further by recognizing that the geostrophic wind shear is a function of the horizontal equivalent potential temperature gradient in a saturated environment. This reduced equation is difficult to evaluate quantitatively because of its dependence on the local value of the moist adiabatic lapse rate. Nevertheless, it shows that horizontal temperature gradients will always act to promote slantwise convection. EPV is a mixture of upright potential instability and slantwise instability. While this is obviously a drawback if one were attempting to assess CSI separately from VPI by combining both instabilities, EPV becomes an all-purpose convection diagnostic tool. EPV is computed from numerical model grids at the National Severe Storms Forecast Center.

1. Introduction

Conditional symmetric instability (CSI) is a significant factor in the evolution of many meteorological events. Slantwise convection, which is the release of CSI, can result in banded, heavy precipitation that cannot be explained through normal synoptic-scale vertical motion processes. Case studies where CSI was important include Sanders and Bosart (1985), Sanders (1986), and Martin et al. (1992). Modica et al. (1994) and Bohorquez and McCann (1995) present a strong case for CSI to modulate conditions present in significant aircraft icing events.

Bennetts and Hoskins (1979) addressed the dynamical theory of CSI, suggesting that it could be a cause of banded precipitation. Emanuel (1983a,b) further expanded the theory to parcel dynamics. Snook (1992) provides an excellent summary of the theory as it applies to operational meteorology. To illustrate how slantwise convection works, these theorists resorted to cross section displays of equivalent potential temperature (θ_e) and a quantity, M_g, defined as absolute geostrophic momentum. Constant M_g surfaces are surfaces of constant inertial stability. A saturated parcel displaced along an M_g surface will maintain its θ_e. If it encounters an environment with lower temperature, that is, when the slope of the θ_e lines are steeper than the M_g lines, it becomes unstable and "convects."

Corresponding author address: Dr. Donald W. McCann, Experimental Forecast Facility, National Severe Storms Forecast Center, Kansas City, MO 64106.

Moore and Lambert (1993) showed how a quantity called equivalent potential vorticity (EPV) can provide quantitative values to assess CSI. They found that cross sections of EPV correctly diagnose zones of banded precipitation. A parcel with negative EPV is convectively unstable, either vertically or slantwise. A positive EPV indicates stable conditions.

Emanuel (1988) asserts that the vorticity due to local flow curvature must be small compared to the Coriolis parameter (f) to find M_g surfaces. Furthermore, Moore and Lambert (1993) explain that the cross section must be carefully chosen normal to the thickness gradient in order to reduce the analysis to two dimensions. Thus, only under restrictions can one examine cross sections for CSI. The problems are obvious. More pragmatically, operational forecasters with large areas of responsibility look at cross sections only if they have the time and motivation to do so. Cross sections may enlighten in many cases, but the time required to find just the right location to place one usually is not the best use of time, given the workload normally placed on these forecasters.

This method cannot assess the horizontal extent of CSI except through the use of multiple cross sections. Operational forecasters would find EPV useful if they could view it "horizontally" as well as in cross section. This note demonstrates that the equation for EPV can be evaluated on quasihorizontal pressure surfaces, forecasts of which most meteorologists receive in gridded form.

2. EPV on pressure surfaces

Martin et al. (1992) and Moore and Lambert (1993) define EPV as

$$\text{EPV} \equiv -g\eta_g \cdot \nabla\theta_e, \tag{1}$$

where g is the gravitational constant, η_g is the three-dimensional (x, y, p) geostrophic absolute vorticity vector, ∇ is the three-dimensional gradient operator, and θ_e is the equivalent potential temperature. Expanding each of the vectors into three dimensions,

$$\text{EPV} = -g\left[\left(\frac{\partial\omega_g}{\partial y} - \frac{\partial v_g}{\partial p}\right)\hat{i} + \left(\frac{\partial u_g}{\partial p} - \frac{\partial\omega_g}{\partial x} + f_j\right)\hat{j} - \left(\frac{\partial v_g}{\partial x} - \frac{\partial u_g}{\partial y} + f_k\right)\hat{k}\right] \cdot \left[\frac{\partial\theta_e}{\partial x}\hat{i} + \frac{\partial\theta_e}{\partial y}\hat{j} - \frac{\partial\theta_e}{\partial p}\hat{k}\right], \tag{2}$$

where the unit vectors, hatted i, j, and k, are in the x, y, and $-p$ (up) directions and u_g, v_g, and ω_g are the x, y, and p geostrophic wind components, respectively. The Coriolis terms are $f_j = 2\Omega\cos\phi$ and $f_k = 2\Omega\sin\phi$. Here $\omega_g = 0$, and the f_j term is small compared with the vertical wind shear terms. Neglecting these terms and carrying out the dot product leads to

$$\text{EPV} = g\left[\frac{\partial\theta_e}{\partial x}\frac{\partial v_g}{\partial p} - \frac{\partial\theta_e}{\partial y}\frac{\partial u_g}{\partial p} - \left(\frac{\partial v_g}{\partial x} - \frac{\partial u_g}{\partial y} + f_k\right)\frac{\partial\theta_e}{\partial p}\right], \tag{3}$$

which is an equation that can be evaluated on gridded data. Combining the first two terms into horizontal vector notation and recognizing that the leading half of the third term is geostrophic absolute vorticity (ζ_g), this equation becomes

$$\text{EPV} = g\left[-\hat{k}\cdot\left(\frac{\partial\mathbf{V}_g}{\partial p} X \nabla_p\theta_e\right) - \zeta_g\frac{\partial\theta_e}{\partial p}\right], \tag{4}$$

where the gradient operator (∇_p) is two-dimensional on a constant pressure surface.

The geostrophic wind shear vector ($\partial\mathbf{V}_g/\partial p$) is the thermal wind. From Emanuel et al. (1987), the relationship between the potential temperature θ and equivalent potential temperature θ_e on a constant pressure surface is

$$\frac{\partial(\ln\theta)}{\partial(\ln\theta_e)} = \frac{\Gamma_m}{\Gamma_d}. \tag{5}$$

In a saturated environment, θ_e may be substituted for θ. The thermal wind equation becomes

$$\frac{\partial\mathbf{V}_g}{\partial p} = \frac{1}{f_k\rho\theta_e}\frac{\Gamma_m}{\Gamma_d}\nabla_p\theta_e \times \hat{\mathbf{k}}. \tag{6}$$

Substituting (6) into (4) and carrying out the vector manipulations leads to

$$\text{EPV} = g\left(-\frac{1}{f_k\rho\theta_e}\frac{\Gamma_m}{\Gamma_d}|\nabla_p\theta_e|^2 - \zeta_g\frac{\partial\theta_e}{\partial p}\right), \tag{7}$$

which is much more difficult to compute, because the moist adiabatic lapse rate varies with both temperature and pressure. However, this form is conceptually simple, because it shows that EPV in a saturated environment is primarily a function of the horizontal and vertical temperature gradients.

The first term on the right-hand side of (7) is *always* less than zero in a saturated environment. The sign of $\partial\theta_e/\partial p$ determines the sign of the second term in (7), because ζ_g is almost always positive. When $\partial\theta_e/\partial p > 0$ (lapse rate steeper than moist adiabatic), the second term becomes negative. Therefore, this term is a measure of upright potential instability.

There are three situations to consider. 1) When the second term is negative, it does not matter how negative the first term is, because upwardly perturbed parcels will become positively buoyant without the release of any inertial instability. 2) When the sounding is strongly stable to moist convection in a weak horizontal temperature gradient, that is, the second term is greater than the absolute value of the first, then all parcels are stable. 3) The more interesting case is when the lapse rate is slightly stable and the horizontal temperature gradient is strong. The large negative value of the first term more than compensates for the small positive value of the second term. This is the case when slantwise convection results. In strong frontal zones, the "slantwise" effect probably plays an important role in developing convective motion in spite of the typical stable lapse rate in the frontal zone. The slantwise effect always "destabilizes" a sounding.

As Moore and Lambert pointed out, EPV is a mixture of upright and slantwise effects. EPV by itself will not tell a forecaster when CSI will occur. For that, a forecaster needs to examine for conditions described in case 3 above. In addition, under conditions described in case 1, EPV will overestimate convective potential because the slantwise effect is never realized.

Emanuel (1983b) and Snook (1992) describe a quantitative assessment of CSI by defining a slantwise convective available potential energy (SCAPE) as the "positive area" between the environmental virtual potential temperature and a "lifted" parcel's virtual potential temperature that follows a constant M_g surface. The accelerations of parcel in a positive SCAPE environment are identical to parcels in a more conventional positive convective available potential energy (CAPE). The only difference between SCAPE and CAPE is the more "horizontal" extent of convective parcels with positive SCAPE. In real atmospheres, CAPEs may become very large, ranging to values greater than 5000 j kg^{-1}. A SCAPE = 500 j kg^{-1} prob-

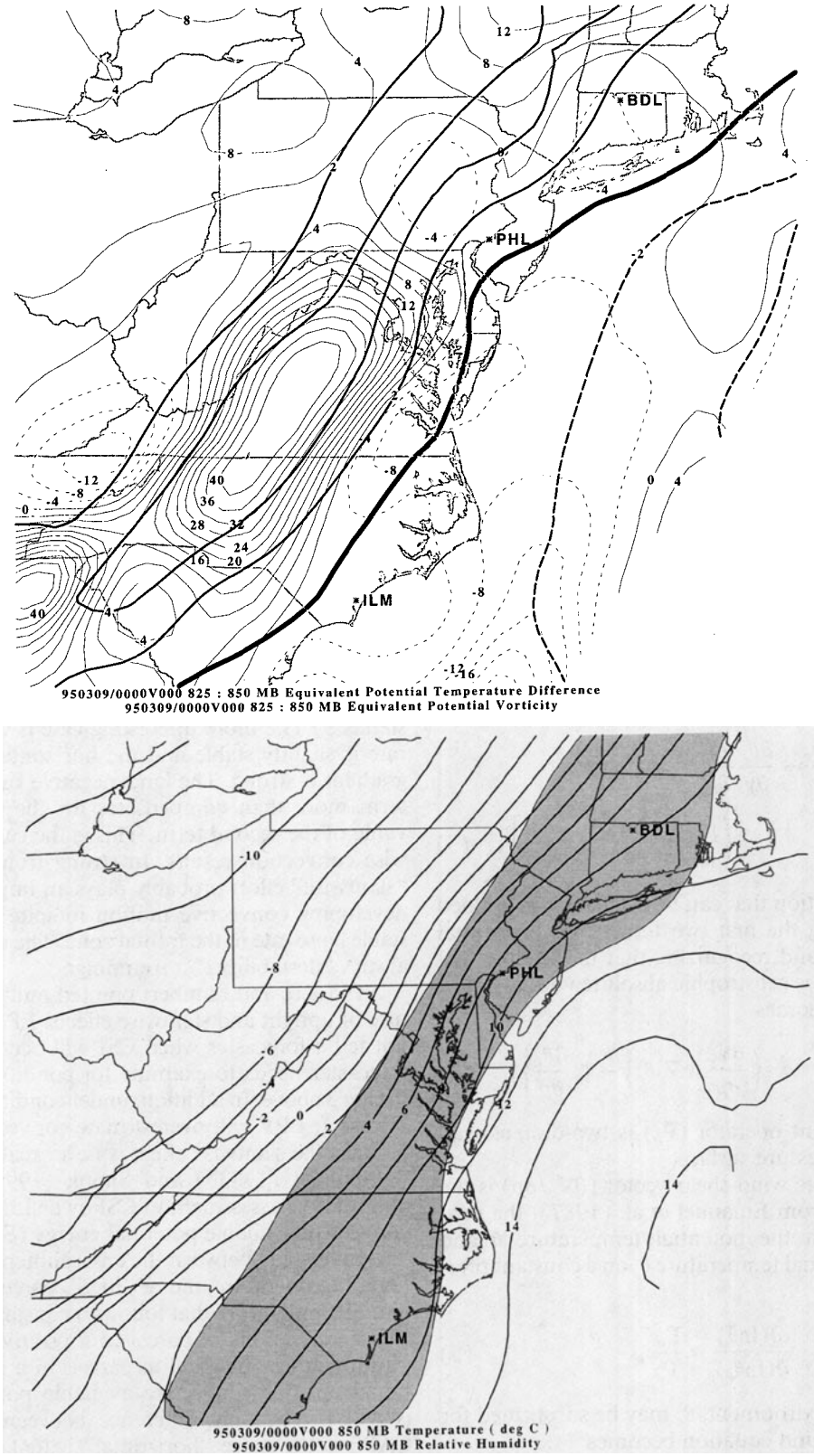

FIG. 1. (a) RUC model analysis for the 825–850-mb layer at 0000 UTC 9 March 1995. Thin contours are EPV in PVU units times 10 with dashed negative contours. Thicker contours are the θ_e difference in the layer with the zero line fattened and negative numbers dashed. (b) RUC model analysis of the 850-mb temperature (black lines) and 850-mb relative humidity > 90% (shaded fill) at the same time.

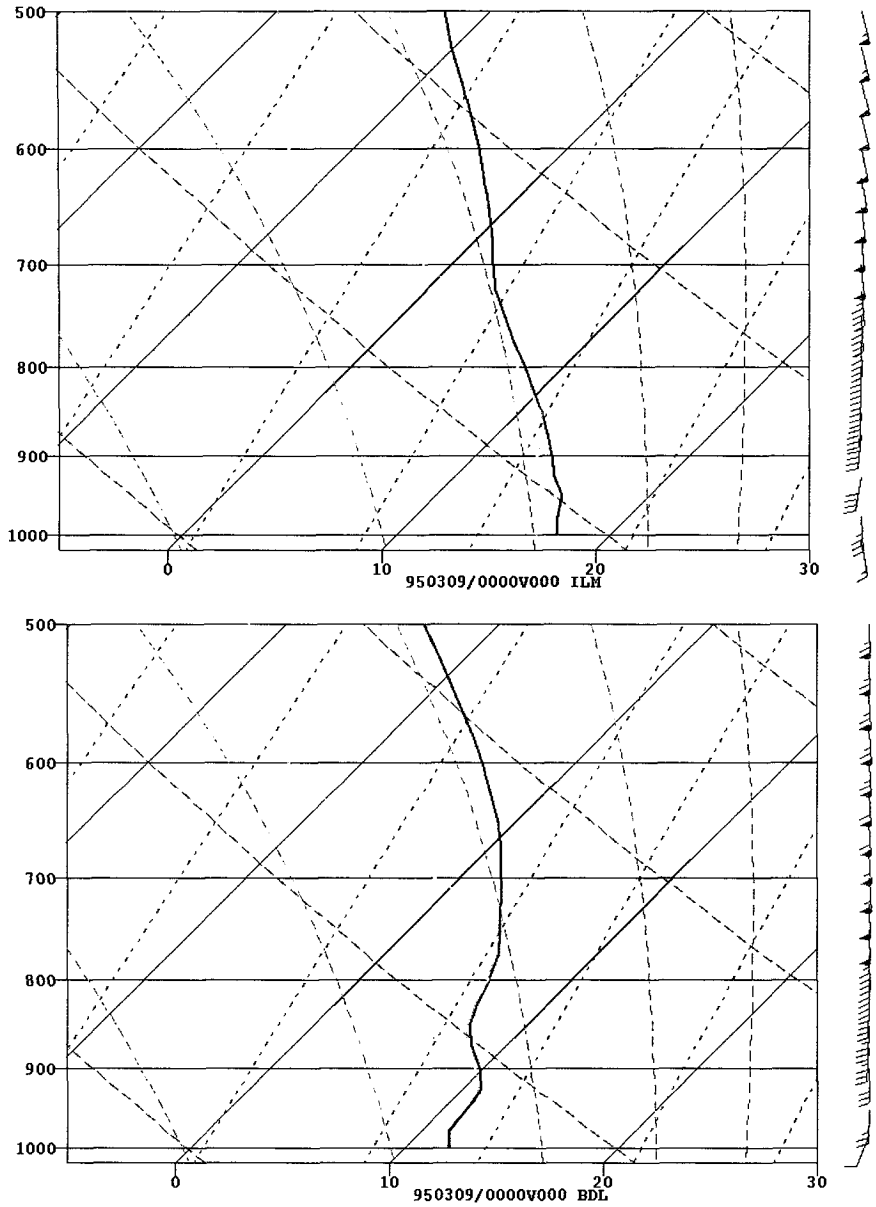

FIG. 2. (a) The 0000 UTC 9 March 1995 RUC model sounding (Skew T–log$p$) for Wilmington, North Carolina (located at ILM in Fig. 1). (b) Same time RUC model sounding for Hartford, Connecticut (BDL in Fig. 1). Temperature profile is in black, while the dewpoint temperature profile is in light gray. Model winds on the right-hand side are in knots.

ably is a very large value (Snook 1992), so in a more practical sense the weather accompanying slantwise convection is usually less intense than weather with vertical convection. However, the effects of equal CAPE and SCAPE are probably about the same, since parcel accelerations are equal. A forecaster may take advantage of EPV's combining convective modes and use it as an all-purpose convection diagnostic tool in a saturated environment. Bohorquez and McCann's (1995) study on aircraft icing is an example of such a combination.

3. Computing EPV

Equation (3) is in a form that can easily accommodate gridded numerical forecast data. EPV can be computed on all numerical model grids at the National Severe Storms Forecast Center. There is one slight modification. Since EPV measures only moist process potential instability, the saturated equivalent potential temperature is substituted for θ_e. Evaluation is only relevant in atmospheric volumes with high relative humidity.

Figure 1a shows an example of the EPV analysis in the 825–850-mb layer on 0000 UTC 9 March 1995 over the mid-Atlantic United States computed from the Rapid Update Cycle (RUC) model analysis. Units are potential vorticity units times 10 (1 PVU = 10^{-6} K m^2 kg^{-1} s^{-1}).

Overlaid on the EPV analysis is the θ_e difference between the two levels. Areas to the south and east of the heavy dark gray line have potentially unstable lapse rates in the vertical sense. Notice the negative EPV values over Connecticut and eastern Pennsylvania that are in the area of potentially stable lapse rates. From Fig. 1b, these negative values correspond to the tight 850-mb temperature gradient. These areas have slantwise convection potential. A check of the 850-mb relative humidity in Fig. 1b shows that slantwise convection is likely because the air is nearly saturated. Indeed, the surface observations at Philadelphia (PHL) reported heavy rain and at Hartford (BDL) moderate rain at this time.

Figure 2a is the model sounding located at Wilmington, North Carolina (ILM). The 850-mb lapse rate is very close to moist adiabatic. The EPV analysis shows slightly negative values over ILM. Since the θ_e decreases a little with height (Fig. 1a), from (4) there is probably little geostrophic wind shear. The model sounding winds reflect that conclusion.

On the other hand, examine the model sounding in Fig. 2b from BDL. The 850-mb lapse rate was quite a bit more stable than in the previous sounding, but the EPV < -0.4 PVU. Since term 2 in (4) is positive, term 1 must have been large negative. Indeed, the temperature gradient on the 850-mb analysis (Fig. 1b) indicates geostrophic wind shear. This second sounding illustrates how horizontal temperature gradients can "destabilize" a sounding. Just looking at these soundings by themselves would mislead a forecaster as to the extent of the convective conditions.

4. Conclusions

Expanding the EPV equation into three dimensions yields a result that simplifies the understanding of when CSI can occur. Moore and Lambert's (1993) analysis of the EPV equation points out that the first term in (7) is generally negative, but by not making the substitution of the horizontal temperature gradient for the geostrophic wind shear, they did not see that this term is always less than zero. The result is that horizontal temperature gradients in saturated environments always promote slantwise convection. The tighter the gradient, the more the slantwise effect will "destabilize" a sounding. The conclusion is that slantwise convection is probably common in frontal zones when the air mass is saturated and vertically potentially stable.

For certain applications, such as aircraft icing diagnostics (Bohorquez and McCann 1995), EPV nicely combines vertical and slantwise potential instabilities and so becomes an all-purpose convective potential tool. For other applications, the knowledge of whether an atmosphere might undergo slantwise or vertical convection may be important. In these cases a forecaster can overlay onto an EPV analysis of the θ_e lapse rate.

This note demonstrates that EPV may be computed on "horizontal" pressure surfaces from gridded numerical data. The resulting analyses and forecasts are easier to digest than cross sections, which are cumbersome to work with and may not be appropriate to the problem. Of course, only analyzing EPV on a single pressure surface does not yield any information about the vertical distribution of conditional instability, which is just as important as its horizontal distribution. Nevertheless, having a three-dimensional EPV analysis at a forecaster's disposal brings new understanding to old forecast problems.

Acknowledgments. Because of Richard Livingston's and anonymous reviewer C's help, I was able to find the relationship between the horizontal temperature gradient and EPV [Eq. (7)], which hopefully will help forecasters better understand moist convective processes. Henry Fields also gave a helpful review. Jim Whistler's graphics work was invaluable.

REFERENCES

Bennetts, D. A., and B. J. Hoskins, 1979: Conditional symmetric instability—A possible explanation for frontal rainbands. *Quart. J. Roy. Meteor. Soc.*, **105,** 945–962.

Bohorquez, M. A., and D. W. McCann, 1995: Model proximity soundings near significant aircraft icing reports. *Proc. Sixth Conf. on Aviation Weather Systems,* Amer. Meteor. Soc., 249–252.

Emanuel, K. A., 1983a: The Lagrangian parcel dynamics of moist symmetric instability. *J. Atmos. Sci.*, **40,** 2368–2376.

——, 1983b: On assessing local conditional symmetric instability from atmospheric soundings. *Mon. Wea. Rev.*, **111,** 2016–2033.

——, 1988: Observational evidence of slantwise convective adjustment. *Mon. Wea. Rev.*, **116,** 1805–1816.

——, M. Fantini, and A. J. Thorpe, 1987: Baroclinic instability in an environment of small stability to slantwise moist convection. Part I: Two-dimensional models. *J. Atmos. Sci.*, **44,** 1559–1573.

Martin, J. E., J. D. Locatelli, and P. V. Hobbs, 1992: Organization and structure of clouds and precipitation on the mid-Atlantic coast of the United States. Part V: The role of an upper-level front in the generation of a rainband. *J. Atmos. Sci.*, **49,** 1293–1303.

Modica, G. D., S. T. Heckman, and R. M. Rasmussen, 1994: An application of an explicit microphysics mesoscale model to a regional icing event. *J. Appl. Meteor.*, **33,** 53–64.

Moore, J. T., and T. E. Lambert, 1993: The use of equivalent potential vorticity to diagnose regions of conditional symmetric instability. *Wea. Forecasting,* **8,** 301–308.

Sanders, F., 1986: Frontogenesis and symmetric stability in a major New England snowstorm. *Mon. Wea. Rev.*, **114,** 1847–1862.

——, and L. F. Bosart, 1985: Mesoscale structure in the megalopolitan snowstorm of 11–12 February 1983. Part I: Frontogenetical forcing and symmetric instability. *J. Atmos. Sci.*, **42,** 1050–1061.

Snook, J. S. 1992: Current techniques for real-time evaluation of conditional symmetric instability. *Wea. Forecasting,* **7,** 430–439.